

Ray travel times in range-dependent acoustic waveguides

Anatoly L. Virovlyansky

*Institute of Applied Physics, Russian Academy of Science,
46 Ul'yanov Street, 603600 Nizhny Novgorod, Russia*

Abstract

The Hamiltonian formalism in terms of the action-angle variables is applied to study ray travel times in a waveguide with a smooth sound speed profile perturbed by a weak range-dependent inhomogeneity. Simple approximate formulas relating the differences in ray travel times to range variations of action variables are derived. By ray tracing in a realistic deep water environment which gives rise to ray chaos, it has been demonstrated that the formulas can be used at ranges up to, at least, 1000 km. The approach considered in this paper gives an insight into mechanisms determining travel time variations. The ray travel time shift due to the perturbation has been decomposed into a sum of two constituents associated with (i) sound speed variations along the trajectory and (ii) variations of a ray trajectory shape. Analytical expressions for these constituents provide a tool for a qualitative and quantitative analysis of timefront variations in the presence of perturbation and shed some light on stability of timefront segments formed by steep rays.

PACS number(s): 43.30.Cq, 43.30.Pc

1 Introduction

The ray travel time is one of the most important and extensively studied characteristics of the wavefield in underwater acoustics. It represents an arrival time of a pulse signal propagating along a ray path connecting the source and the observation point. In field experiments such pulses, especially those propagating through steep ray paths, can often be resolved and identified even at ranges of hundreds km and longer. In many schemes of acoustic monitoring of ocean structure, ray travel times are main observables used to reconstruct variations in the environment [1, 2].

In the past decade it has been realized that ocean inhomogeneities (such as internal waves) give rise to ray chaos [3]-[9]. Numerical calculations have demonstrated that if a smooth sound speed profile is perturbed with a range-dependent inhomogeneity, then ray paths (or some of them) reveal extreme

sensitivity to initial conditions. Trajectories which are initially neighbors move apart at an exponential rate and the number of eigenrays increases exponentially with range. It might be expected that under these conditions the structure of ray arrivals becomes unpredictable and quite different from that in the unperturbed waveguide.

However, it turns out that travel times of rays in the perturbed and unperturbed waveguides have common features. As it was discovered numerically by Tappert and Tang [8] (see also Ref. [10]), in the presence of perturbation the eigenray splits into a cluster of new eigenrays with travel times closely spaced in the vicinity of the unperturbed arrival. In this sense, ray travel times turn out to be stable characteristics of the wave field. This property also manifests itself in comparative stability of early portions of timefronts (ray arrivals in depth-time plane) formed by steep rays [9, 11, 12]. These facts suggest that travel time variations of even chaotic rays may be described using some perturbation theory.

In this paper we argue that rather simple analytic relations for description of ray travel time variations can be obtained by applying the Hamiltonian formalism [3, 6, 8, 9] and expressing the ray characteristics via the so-called action-angle canonical variables [3, 14]. The action variable, I , defines the shape of a cycle of the ray path while the angle variable, θ , indicates the position of a current ray point inside the cycle.

We study the difference in travel times, Δt , for a pair of rays starting at close launch angles from the points set at close depths. It is assumed that these rays arrive at, generally other, two points with also close depths and at close arrival angles. In other words, the trajectories start from two points closely spaced in phase space and arrive at other two closely spaced points. Both trajectories propagate over the same range interval but they can have **different** numbers of cycles. It is clear that differences in action variables, ΔI , of the trajectories are small at the initial and final ranges. Assuming that ΔI remains to be small at intermediate ranges as well, we expand the expression for Δt in ΔI and drop terms $O(\Delta I^3)$. In so doing we restrict ourselves to not very long propagation ranges. Nevertheless, our numerical simulations show that this approximation works well up to, at least, 1000 km range (longer ranges have not yet been considered).

Our main objective is to demonstrate that the use of the action-angle variables can significantly simplify the analysis of ray travel times. In particular, we show that a simple evaluation of the action, I , as a function of the launch angle, χ_0 , in a range-independent waveguide provides a lot of quantitative information on difference in ray travel times. The function $I(\chi_0)$ determines the temporal shifts between neighboring segments of the timefront at arbitrary range.

The perturbation approach considered in this paper gives an insight into mechanisms affecting ray travel times in the presence of a weak perturbation “responsible” for chaotic ray dynamics. The travel time shift due to the perturbation is decomposed here into a sum of two simple analytic expressions: one term accounts for the time delay due to sound speed variations along the trajectory while another term describes the time shift due to variations of a

ray trajectory shape. This formalism is convenient for estimating an averaged travel time bias caused by inhomogeneities.

In Section 2, a brief description of the Hamiltonian formalism in terms of the position-momentum and action-angle canonical variables is given. Approximate relations for differences in ray travel times are derived in Section 3. Three types of relations have been obtained. They allow one to compare travel times of (i) two rays in a waveguide with a smooth (unperturbed) range-independent sound speed profile, (ii) two rays in the same waveguide with a weak range-dependent perturbation, and (iii) one ray in an unperturbed waveguide and another one in a perturbed waveguide. Section 4 contains results of numerical simulation carried out for a model of a stratified waveguide perturbed with range-dependent inhomogeneities induced by internal waves. It is demonstrated that our approximate formulas give rather accurate predictions at 1000 km range. The mechanisms leading to dispersion and shift of individual branches (segments) of the timefront in the presence of inhomogeneities have been examined. It has been found that, for most rays, travel time shifts due to variations in ray trajectory shapes dominate over variations caused by sound speed fluctuations along the trajectory. In Section 5 we shortly outline the generalization of our approach to the model in which the unperturbed waveguide adiabatically varies with range. In Section 6 the results of this work are summarized.

The Appendix contains the main formulas defining the Hamiltonian formalism for a ray theory in the parabolic equation (small-angle) approximation.

2 Hamiltonian formalism

In this Section we describe the Hamiltonian formalism corresponding to the ray theory derived from the full wave equation [3, 6, 9, 15, 16]. We present explicit expressions defining the Hamiltonian, action function (eikonal), ray equations and canonical transformation from the position-momentum to action-angle variables. Similar expressions for the Hamiltonian formalism corresponding to the parabolic equation (small-angle) approximation are given in the Appendix.

2.1 Ray equations in terms of position-momentum variables

Consider wave propagation in a two-dimensional medium with the coordinates r (range) and z (depth). It is assumed that the z -axis is directed downward and the plane $z = 0$ is the sea surface. The ray trajectory $z(r)$ is determined by the sound speed field $c(r, z)$ and can be found from Fermat's principle [15, 16] according to which the first variation of the functional

$$S = \bar{c} \int \frac{ds}{c(r, z)} = \int dr n(r, z(r)) \sqrt{1 + \left(\frac{dz}{dr}\right)^2}, \quad (1)$$

vanishes at the ray trajectory. Here $n(r, z) = \bar{c}/c(r, z)$ is the refractive index, \bar{c} is a reference sound speed, and $ds = dr \left(1 + (dz/dr)^2\right)^{1/2}$ is the arc length. The functional S represents the so-called eikonal and it relates to the ray travel time by

$$t = S/\bar{c}. \quad (2)$$

Formally considering Eq. (1) as an action function of some mechanical system with the r -variable playing the role of time, one can apply the standard relations of classical mechanics [13]-[15]. This yields explicit expressions for the momentum,

$$p = n \frac{dz/dr}{\sqrt{1 + (dz/dr)^2}}, \quad (3)$$

and the Hamiltonian,

$$H = -\sqrt{n^2 - p^2}. \quad (4)$$

Equations $p = n \sin \chi$ and $H = -n \cos \chi$ relate the momentum and the Hamiltonian to the ray grazing angle, χ [9].

Expression (1) for the eikonal can now be rewritten as

$$S = \int (pdz - Hdr). \quad (5)$$

Ray trajectories are governed by the Hamilton equations [8, 9, 14]

$$\frac{dz}{dr} = \frac{\partial H}{\partial p} = -\frac{p}{H} = \frac{p}{\sqrt{n^2 - p^2}}, \quad (6)$$

$$\frac{dp}{dr} = -\frac{\partial H}{\partial z} = \frac{n \partial n / \partial z}{\sqrt{n^2 - p^2}}. \quad (7)$$

Equation (1)-(7) present the Hamiltonian formalism in terms of the momentum-position canonical variables. In the remainder of this section we introduce another pair of canonically conjugated variables, namely, the action-angle variables [3, 14, 13, 16].

2.2 Action-angle variables

2.2.1 Range-independent waveguide

First, we define the action-angle variables in a range-independent waveguide with $c = c_0(z)$ and, correspondingly, $n = \bar{c}/c_0(z) = n_0(z)$. In such a waveguide the Hamiltonian remains constant along the ray trajectory:

$$H_0 = -\sqrt{n_0^2(z) - p^2} = -n_0(z) \cos \chi = \text{const}. \quad (8)$$

This is Snell's law [17, 18] analogous to the energy conservation law in classical mechanics. Equation (8) establishes a simple relation between the momentum p and coordinate z

$$p = \pm \sqrt{n_0^2(z) - H_0^2}. \quad (9)$$

The action variable I is defined as the integral [3, 13, 14]

$$I = \frac{1}{2\pi} \oint p dz = \frac{1}{\pi} \int_{z_{\min}}^{z_{\max}} dz \sqrt{n_0^2(z) - H_0^2} \quad (10)$$

running over the cycle of ray trajectory. Here z_{\min} and z_{\max} are the depths of upper and lower ray turning points, respectively. Equation (10) determines "energy", H_0 , as a function of the action variable, I . Note the relation

$$\frac{dH_0}{dI} = \frac{2\pi}{D} = \omega, \quad (11)$$

where

$$D = -2H_0 \int_{z_{\min}}^{z_{\max}} \frac{dz}{\sqrt{n_0^2(z) - H_0^2}} \quad (12)$$

is the cycle length of the ray path, and ω is the angular frequency of spatial path oscillations. Equation (12) follows from (6), (9), and (10).

The canonical transformation from the position-momentum, (p, z) , to the action-angle, (I, θ) , variables

$$I = I(p, z), \quad \theta = \theta(p, z) \quad (13)$$

and the inverse transformation

$$z = z(I, \theta), \quad p = p(I, \theta) \quad (14)$$

are determined by the equation [14]

$$dS = pdz - H_0 dr = dG - \theta dI - H_0 dr, \quad (15)$$

where $G = G(I, z)$ is the generating function. An explicit expression for $G(I, z)$ is well-known [3, 14]. We represent it in the form

$$G(I, z) = \begin{cases} \int_{z_{\min}}^z dz \sqrt{n_0^2(z) - H_0^2(I)}, & p > 0 \\ 2\pi I - \int_{z_{\min}}^z dz \sqrt{n_0^2(z) - H_0^2(I)}, & p < 0 \end{cases}, \quad (16)$$

where z_{\min} and z_{\max} are considered as functions of I . Then the pair of coupled equations

$$p = \frac{\partial G}{\partial z} = \pm \sqrt{n_0^2(z) - H_0^2(I)}, \quad (17)$$

$$\theta = \frac{\partial G}{\partial I} = \begin{cases} -\frac{2\pi H_0(I)}{D} \int_{z_{\min}}^z \frac{dz}{\sqrt{n_0^2(z) - H_0^2(I)}}, & p > 0 \\ 2\pi + \frac{2\pi H_0(I)}{D} \int_{z_{\min}}^z \frac{dz}{\sqrt{n_0^2(z) - H_0^2(I)}}, & p < 0 \end{cases} \quad (18)$$

defines all the four functions in Eqs. (13) and (14).

Note, that the so defined angle variable θ varies from 0 to 2π at a part of the trajectory beginning at one minimum and ending at the next one. To make the action variable continuous, its value should be increased by 2π at the beginning of each new cycle. Here we assume that the cycle begins at the minimum of the trajectory. It should be emphasized that both functions in Eq. (14) are periodic in θ with period 2π .

The ray equations in the new variables take the trivial form

$$\frac{dI}{dr} = -\frac{\partial H_0}{\partial \theta} = 0, \quad \frac{d\theta}{dr} = \frac{\partial H_0}{\partial I} = \omega(I) \quad (19)$$

with the solution

$$I = I_s, \quad \theta = \theta_s + \omega(I_s) r, \quad (20)$$

where I_s and θ_s are starting values of the action and angle variables, respectively, at $r = 0$.

An explicit expression for the action function (eikonal) is obtained by integrating Eq. (15). For a ray connecting points $(0, z_s)$ and (r, z_e) , after some algebra we get

$$S = (I_s \omega(I_s) - H_0(I_s)) r - G(z_s, I_s) + G(z_e, I_s) + I_s (\theta_s - \theta_e), \quad (21)$$

where θ_s and θ_e are angle variables at ranges 0 and r , respectively, and the value of θ_e is taken modulo 2π (θ_s never exceeds 2π). The subscript 's' marks ray parameters at $r = 0$ while 'e' marks parameters at the end of the trajectory. This convention will be used throughout the paper. The symbol θ_e will always designate the final value of the angle variable modulo 2π . The angle variable at the end point, θ , is related to θ_s and θ_e by

$$\theta = 2\pi N - \theta_s + \theta_e, \quad (22)$$

where N is an integer equal to the number of cycles of the ray path.

Let us emphasize an almost trivial, but crucial for our subsequent analysis, point. Canonical transformations (13) and (14) determined by the function $n_0(z)$, formally, can be applied in a waveguide with a different refractive index profile.

2.2.2 Range-dependent waveguide

In what follows we shall consider a model of sound speed field taken in the form

$$c(r, z) = c_0(z) + \delta c(r, z), \quad (23)$$

where $c_0(z)$ is a smooth (background) sound speed profile, and $\delta c(r, z)$ is a range-dependent perturbation. In this range-dependent environment where the refractive index, $n = \bar{c}/c$, is a function of both range and depth, we define the action-angle variables using the **same** relations as in the unperturbed waveguide with the refractive index $n_0(z) = \bar{c}/c_0(z)$.

Rewrite the Hamiltonian $H = -\sqrt{n^2 - p^2}$ in the form

$$H = H_0 + V, \quad (24)$$

where

$$\begin{aligned} H_0(p, z) &= -\sqrt{n_0^2(z) - p^2}, \\ V(p, z, r) &= -\sqrt{n^2(z, r) - p^2} + \sqrt{n_0^2(z) - p^2}. \end{aligned} \quad (25)$$

Since our generating function G does not depend explicitly on r , the Hamiltonian in the new variables (I, θ) is obtained by simple substitution of functions (14) into the above equations. This yields

$$H(I, \theta, r) = H_0(I) + V(I, \theta, r). \quad (26)$$

The action function (eikonal), S , again can be found by integrating Eq. (15) with H_0 changed to H . Then we arrive at

$$S = \int (I d\theta - H dr) - G(z_s, I_s) + G(z_e, I_e) + \theta_s I_s - \theta_e I_e. \quad (27)$$

Note, that Eq. (22) remains valid in a range-dependent waveguide.

The Hamilton equations now take the form

$$\frac{dI}{dr} = -\frac{\partial V}{\partial \theta}, \quad (28)$$

and

$$\frac{d\theta}{dr} = \omega + \frac{\partial V}{\partial I}. \quad (29)$$

The following two comments should be made to this definition of the action-angle variables.

(i) The action variables introduced in this way (we have followed Refs. [3, 16]) do not conserve along the ray path even in a waveguide smoothly varying with range, i.e. our actions are not adiabatic invariants. Another definition of these variables [14] where the action does have a property of adiabatic invariance is shortly described in Section 5.

(ii) Splitting of the Hamiltonian into a sum of the unperturbed constituent, H_0 , and the perturbation, V , have been made in anticipation of our later use of some perturbation expansion based on smallness of δc and, hence, V . However, for now we have not assumed the perturbation to be small and all the equations derived so far are exact.

3 Travel time differences

In this section we examine the difference in eikonals (travel times) for a pair of rays starting from two *close* points in the phase plane (p, z) (or (I, θ)), and arriving at, generally, other two *close* points. These rays may have different numbers of cycles of oscillations.

To distinguish between similar parameters of these two rays, parameters of one of them will be marked with overbar. For example, starting and final points of one trajectory will be denoted by (p_s, z_s) and (p_e, z_e) , respectively, while for another trajectory we shall write (\bar{p}_s, \bar{z}_s) and (\bar{p}_e, \bar{z}_e) .

The symbol Δ will be used to denote the difference between any characteristic of one ray and its counterpart for another ray, e.g. $\Delta I = I - \bar{I}$, $\Delta S = S - \bar{S}$, $\Delta z_s = z_s - \bar{z}_s$, and so on. The mean value of some ray parameter and its counterpart for another ray will be designated with tilde over the corresponding symbol. In particular, $\tilde{I} = (I + \bar{I})/2$.

3.1 Two rays in a range-independent waveguide

Let us begin with a pair of rays in the unperturbed waveguide with $n = n_0(z)$. Rewrite Eq. (21) as

$$S = F(I)r - G(z_s, I) + G(z_e, I) + I(\theta_s - \theta_e), \quad (30)$$

where

$$F(I) = I\omega(I) - H_0(I). \quad (31)$$

In this case $I_s = I_e$ and we have dropped the subscript at I . It follows from Eq. (11) that

$$F' = I\omega', \quad F'' = \omega' + I\omega'', \quad (32)$$

where the prime denotes differentiation with respect to I . Later on, the prime will be also used to denote a partial derivative with respect to I .

The closeness of starting parameters of our rays ensures that the difference ΔI is small, and in the expansion

$$F(I) - F(\bar{I}) = \omega'(\tilde{I})\Delta I + O(\Delta I^3) \quad (33)$$

we retain only the first term.

If we expand ΔS in a Taylor series about \tilde{I} , \tilde{z}_s , \tilde{z}_e , $\tilde{\theta}_s$, and $\tilde{\theta}_e$ and retain only first order terms in small differences ΔI , Δz_s , Δz_e , $\Delta \theta_s$, and $\Delta \theta_e$, then we obtain

$$\Delta S = \tilde{I}\omega'(\tilde{I})r\Delta I - \tilde{p}_s\Delta z_s + \tilde{p}_e\Delta z_e + \tilde{I}(\Delta\theta_s - \Delta\theta_e). \quad (34)$$

In the same approximation Eqs. (20) and (22) yield

$$\Delta\theta = \omega'(\tilde{I})r\Delta I = 2\pi\nu - (\Delta\theta_s - \Delta\theta_e), \quad (35)$$

where $\nu = N - \bar{N}$ is the difference in numbers of cycles for the two ray trajectories. Substituting Eq. (35) into Eq. (8) we get

$$\Delta S = 2\pi\nu\tilde{I} - \tilde{p}_s\Delta z_s + \tilde{p}_e\Delta z_e. \quad (36)$$

When deriving this approximate relation, we have dropped terms proportional to r , and it may seem that Eq. (36) is valid only at short enough ranges. However, it is not so. The point is that the terms proportional to r dropped in

Eqs. (34) and (35) are, on the other hand, proportional to ΔI^3 (see Eq. (33)). According to Eq. (35), the difference ΔI can be estimated as

$$\Delta I \sim \frac{2\pi\nu}{\omega'r}$$

and this estimation shows that if ν is kept constant then the neglected terms not increase, but decrease with range.

In the case of $\Delta z_s = \Delta z_e = 0$, i.e. for two eigenrays connecting points $(0, z_s)$ and (r, z_e) , Eq. (36) reduces to

$$\Delta S = 2\pi\nu\tilde{I}. \quad (37)$$

This result is known (see Refs. [19]-[21]). In Refs. [19, 21] it has been shown that Eq. (37) remains valid in a waveguide adiabatically varying with range.

3.2 Two rays in a range-dependent waveguide

Now turn our attention to a pair of rays in a range-dependent waveguide with sound speed spatial distribution (23). Representing Eq. (29) in the form

$$d\theta = (\omega + V') dr \quad (38)$$

and substituting it into Eq. (27) we obtain

$$S = \int F(I) dr + \int (IV' - V) dr - G(z_s, I) + G(z_e, I) + I_s\theta_s - I_e\theta_e. \quad (39)$$

Since starting points of our rays are closely spaced in the phase space and the same is true of their end points, the value of ΔI is small at the beginning and at the end of the considered range interval. Assuming the perturbation V to be small we restrict ourselves to not very long distances where $|\Delta I|$ remains small enough at intermediate ranges and again retain only the first term in expansion (33).

Then the difference in eikonals up to the first order terms in the same small differences that have been considered when deriving Eq. (36), can be presented in the form

$$\begin{aligned} \Delta S = & \int \tilde{I}\omega'(\tilde{I})\Delta I dr + \int (V - \bar{V})dr + \int (IV' - \bar{I}\bar{V}') dr \\ & - \tilde{p}_s\Delta z_s + \tilde{p}_e\Delta z_e + \tilde{I}_s\Delta\theta_s - \tilde{I}_e\Delta\theta_e. \end{aligned} \quad (40)$$

A further simplification of this equation depends on relative values of different terms on the right hand side. First of all, it is clear that the differences Δz_s , Δz_e , $\Delta\theta_s$, and $\Delta\theta_e$, and, hence, the last four terms in (40), can be made very small by imposing strong enough restrictions on ray parameters at the beginning and at the end of the trajectories. On the other hand, contributions from the three other terms, on average, should grow with range.

In the next Section we check numerically two simplified versions of Eq. (40). One of them, obtained by retaining only the first two terms on the right, is given by

$$\Delta S = \int \tilde{I}\omega'(\tilde{I})\Delta I dr + \int (V - \bar{V})dr. \quad (41)$$

Although neglecting the term

$$\int (IV' - \bar{I}\bar{V}') dr$$

looks somewhat arbitrary, numerical results presented later on show that Eq. (41) give a reasonable approximation to ΔS for rays with different numbers of cycles.

Another simplified version of Eq. (40) can be obtained by representing the final difference in angle variables in two forms (on the analogy of Eq. (35))

$$\Delta\theta = \int \omega'(\tilde{I})\Delta I dr + \int (V' - \bar{V}') dr = 2\pi\nu - (\Delta\theta_s - \Delta\theta_e), \quad (42)$$

and assuming that \tilde{I} does not deviate substantially from its range averaged value $\langle \tilde{I} \rangle$. We approximately replace $\tilde{I}_s\Delta\theta_s - \tilde{I}_e\Delta\theta_e$ by $\langle \tilde{I} \rangle (\Delta\theta_s - \Delta\theta_e)$ and, similarly, neglect the difference between $\int (IV' - \bar{I}\bar{V}') dr$ and $\langle \tilde{I} \rangle \int (V' - \bar{V}') dr$. Then, from Eqs. (40) and (42) we get

$$\begin{aligned} \Delta S = 2\pi\nu \langle I \rangle + \int (\tilde{I} - \langle I \rangle)\omega'(\tilde{I})\Delta I dr + \int (V - \bar{V})dr \\ - \tilde{p}_s\Delta z_s + \tilde{p}_e\Delta z_e. \end{aligned} \quad (43)$$

As we shall see, this more sophisticated estimation gives a better prediction of travel time differences.

3.3 Ray in a range-independent waveguide and ray in a range-dependent waveguide

To find out how the presence of small range-dependent component of the sound speed, $\delta c(r, z)$, affects travel times, we compare a pair of rays one of which propagates in a range-independent waveguide (its parameters will be marked with the overbar) and another one propagates in a range-dependent waveguide. Once again, it is assumed that the ray starting points are closely spaced in phase plane and the same is true of their arrival points. Both rays propagate over the same range interval.

By subtracting Eq. (30) from Eq. (39) we obtain the difference in eikonals, ΔS , that can be simplified in the same manner as it has been done above. However, we use here expansions about parameters of the ray propagating in a range-independent waveguide, but not about mean values of analogous parameters for the two rays. Expanding $F(I)$ in Eq. (39) in a Taylor series about \bar{I} and neglecting terms $O(\Delta I^3)$ yields

$$\begin{aligned} \Delta S = \int \left(\bar{I}\omega'(\bar{I})\Delta I + \frac{1}{2}(\omega'(\bar{I}) + \bar{I}\omega''(\bar{I})\Delta I^2) \right) dr - \int (V - IV')dr \\ + \bar{p}_e\Delta z_e - \bar{p}_s\Delta z_s + \bar{I}(\Delta\theta_s - \Delta\theta_e), \end{aligned} \quad (44)$$

where only first order terms in small differences Δz_s , Δz_e , $\Delta\theta_s$, and $\Delta\theta_e$ have been retained.

Similarly, the difference in angle variables is given by

$$\Delta\theta = 2\pi N - \Delta\theta_s + \Delta\theta_e = \int \left(\omega'(\bar{I})\Delta I + \frac{1}{2}\omega''(\bar{I})\Delta I^2 + V' \right) dr. \quad (45)$$

By combining the above two equations and neglecting the term

$$\Delta S_{negl} = \int V' \Delta I dr, \quad (46)$$

we obtain

$$\Delta S = 2\pi N\bar{I} + \bar{p}_e\Delta z_e - \bar{p}_s\Delta z_s + \frac{1}{2} \int \bar{\omega}' \Delta I^2 dr - \int V dr. \quad (47)$$

Establishing of applicability conditions of approximate relations given in Eqs. (36), (41), (43) and (47) requires estimations of neglected terms. The detailed analysis of this issue is beyond the scope of the present paper but in the next Section, with an example of a realistic propagation model, we demonstrate that these relations can give good predictions at up to, at least, 1000 km ranges.

4 Numerical example and discussion

4.1 Environmental model

The unperturbed sound speed profile $c_0(z)$ used in our numerical simulation is shown in the left panel of Fig. 1. Its minimum (sound-channel axis) is located at the depth $z_a = 0.738$ km. Our model of $\delta c(r, z)$ is close to that exploited in Ref. [9]. It represents the sound speed perturbation due to a field of internal waves and is defined by the relation

$$\delta c(r, z) = Q e^{-3z/2B} \sum_{j=1}^{10} A_j \sin(j\pi e^{-z/B}) \cos(j\kappa r + \phi_j). \quad (48)$$

Each term in the sum models a contribution from one of ten internal wave modes taken in the WKB approximation [22]. The phases, ϕ_j , are distributed uniformly over the interval $(0, 2\pi)$, and dimensionless random amplitudes are weighted according to

$$\langle A_j^2 \rangle = 1/(j^2 + j_*^2),$$

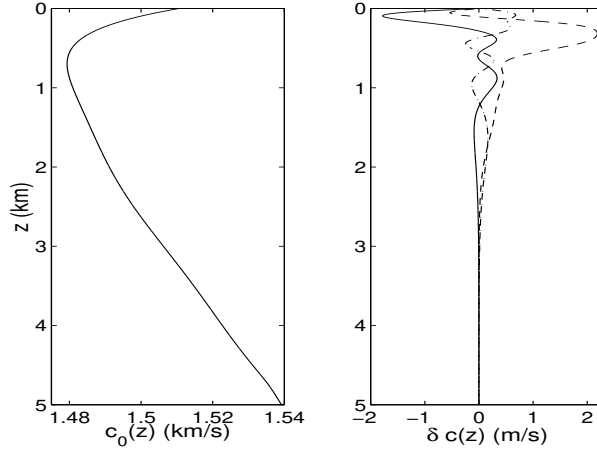


Fig.1. *Left panel*: Unperturbed sound speed profile. *Right panel*: Sound speed perturbations at three different ranges.

where $j_* = 3$. The constants κ and B , defining horizontal wavenumbers of internal wave modes and a depth dependence of buoyancy frequency, respectively, have the values: $\kappa = 2\pi/75$ 1/km, $B = 1$ km. With this value of κ the function $\delta c(r, z)$ is periodic in range with a period of 75 km. In our numerical simulation only one realization of the internal wave field has been used. The constant Q has been selected equal to 0.03 km/s. Then the rms magnitude of sound speed fluctuations, δc , near the surface is about 1 m/s. Depth dependences of δc at three different ranges are presented in the right panel of Fig. 1.

The angular frequency of ray trajectory oscillations in the unperturbed waveguide, ω , and its derivative with respect to the action variable are shown in Fig. 2 as functions of I .

4.2 Timefront

The upper panel in Fig. 3 shows the timefront (ray arrivals in the depth-time plane) in the unperturbed waveguide. It has been computed at 1000 km range using a fan of 4500 rays escaping from the point source set at the depth $z = z_a$ with starting momenta equally spaced within the interval corresponding to launch angles $\pm 10^\circ$. A timefront at 1000 km range in the perturbed waveguide is shown in the lower panel of Fig. 3. This plot has been produced by tracing 18000 rays escaping the same point source with starting momenta uniformly incremented within the same interval. In both perturbed and unperturbed waveguides the fan rays do not strike the sea surface at $z = 0$.

The timefront in the range-independent waveguide has the well-known accordion-like shape consisting of smooth segments (branches). Each segment is formed by points corresponding to arrivals of rays with the same identifier $\pm J$, where \pm is the sign of launch angle and J is the number of ray turning points. Segments formed by rays with the same sign of the launch angle and close values of J

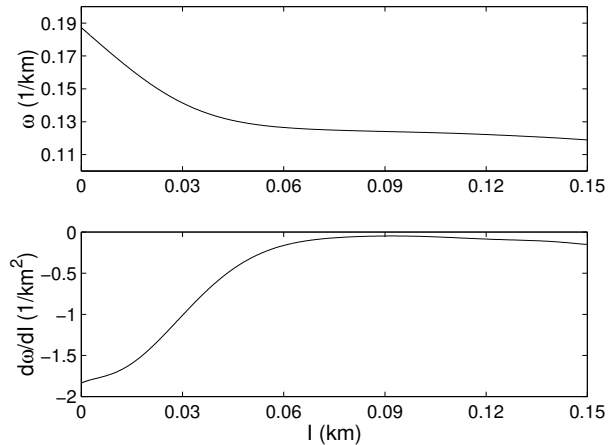


Fig. 2. Angular frequency of ray oscillations, ω , (upper panel) and its derivative with respect to the action variable, $d\omega/dI \equiv \omega'$, (lower panel) versus the action variable I for rays propagating without striking the surface and the bottom.

are almost parallel. The intervals between such segments along the t -axis are important characteristics of temporal structure of the pulse signal.

Equations (36) and (37) provide a convenient tool for estimating these intervals. To illustrate this point, consider the segments formed by rays with positive launch angles (starting downward) and odd numbers of turning points. All such segments in Fig. 3 are marked by numbers indicating the corresponding values of J . At each of these segments we choose a point with the largest value of z , i.e. a point at the lower end of the segment, and denote the travel time of the corresponding ray by t_J . With Eq. (36) we estimate differences $t_J - t_{J-2}$ characterizing temporal shifts between neighboring segments. When applying Eq. (36) we must take $\nu = 1$, because rays with the identifiers $+(J-2)$ and $+J$ have numbers of cycles that differ by 1. In Table 1 the estimations of differences $t_J - t_{J-2}$ predicted by Eq. (36) (central column) are compared to their exact values (right column) obtained by direct ray tracing. This comparison demonstrates a high accuracy of estimation (36).

An interesting and somewhat surprising fact following from (36) is that there exists a conservation law for temporal shifts between the timefront segments. Consider a bunch of rays with launch angles within a narrow interval. Action variables of all these rays are close to some value that we denote by I_0 . Beginning from a certain range r_* these rays will form at least two segments of the timefront with identifiers differing by 2. When estimating temporal shift between two such segments we should compare rays arriving at the same depths, i.e. the eigenrays, and so, we can apply Eq. (37) instead of Eq. (36). With this in mind, we can estimate the temporal shift as $\tau_0 = 2\pi I_0/\bar{c}$. It should be emphasized that τ_0 does **not** depend on range. It means that although the number of segments formed by rays with launch angles from a narrow angular interval

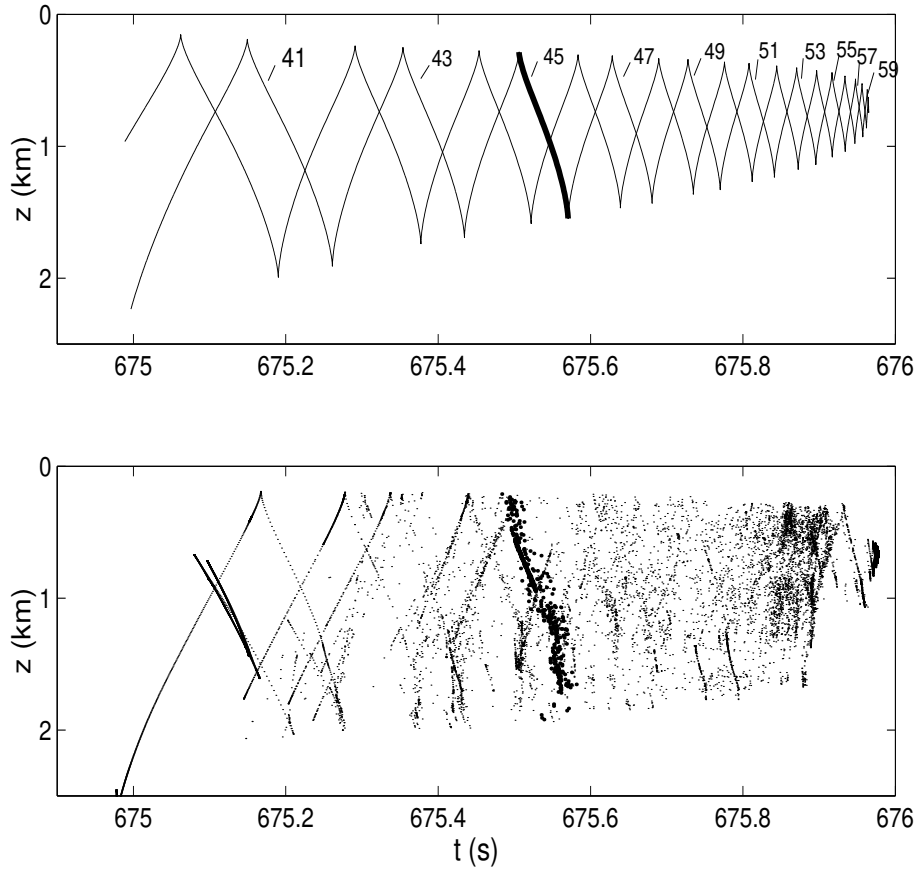


Fig. 3. Timefront for 1000 km propagation without (upper panel) and with (lower panel) internal waves present. Time front segments in the upper panel formed by rays starting downward and having odd numbers of turning points are marked with numbers. Each number indicates the absolute value of identifier, J , (number of turning points) for the corresponding segment. Arrivals with the identifier $J = +45$ are depicted by solid line in the upper and by large points in the lower.

J	$t_J - t_{J-2}$ (s), approx	$t_J - t_{J-2}$ (s), exact
43	0.1764	0.1732
45	0.1368	0.1360
47	0.1106	0.1103
49	0.0896	0.0894
51	0.0712	0.0712
53	0.0545	0.0544
55	0.0385	0.0385
57	0.0229	0.0231
59	0.0082	0.0077

Table 1: Differences in travel times of rays forming the lower ends of timefront segments corresponding to identifiers $+J$ and $+(J-2)$. *Central column*: predicted by Eq. (37). *Right column*: ray tracing result.

grows linearly with range, temporal shifts between neighboring segments (to be more precise, between segments corresponding to identifiers $\pm J$ and $\pm(J-2)$) remain approximately the same at any distance. It is quite clear that analogous statement is true of differences in travel times of eigenrays. A more detailed discussion of this issue is given in Refs [19, 21].

It may seem unexpected, but a simple evaluation of the action variable as a function of launch angle gives a considerable quantitative information on temporal structure of the pulse signal, and, moreover, this information is valid at any (long enough) range. Figure 4 shows the dependence of

$$\tau = 2\pi I/\bar{c} \tag{49}$$

on the launch angle χ . Looking at this curve we can predict that, for example, a difference in travel times of two eigenrays with launch angles close to 6° and numbers of cycle differing by 1, will be close to $\tau = 0.15$ s at **any** range and at **any** depth, provided such eigenrays arrive at the observation point.

In the presence of weak range-dependent inhomogeneities the structure of timefront becomes much more complicated: instead of infinitely thin segments of smooth curves, we have some areas filled with randomly scattered points. Although we observe the scattered points only because our fan is far too sparse to resolve what should be unbroken curves, the appearance of such regions indicates the presence of chaotic rays.

In spite of the destruction caused by the perturbation, the early portion of the timefront formed by steep rays still “remembers” some of its features in the unperturbed waveguide. The points depicting arrivals of rays with the given identifier are scattered in the vicinity of the unperturbed segment corresponding to the same identifier. Loosely, steep chaotic rays produce a fuzzy version of the pattern typical of the range-independent waveguide [9, 11]. For example, compare the fragments of the timefronts in the unperturbed and perturbed waveguides formed by rays with the identifier $+45$. They are depicted by a thick solid line in the upper panel of Fig. 3 and by large points in the lower

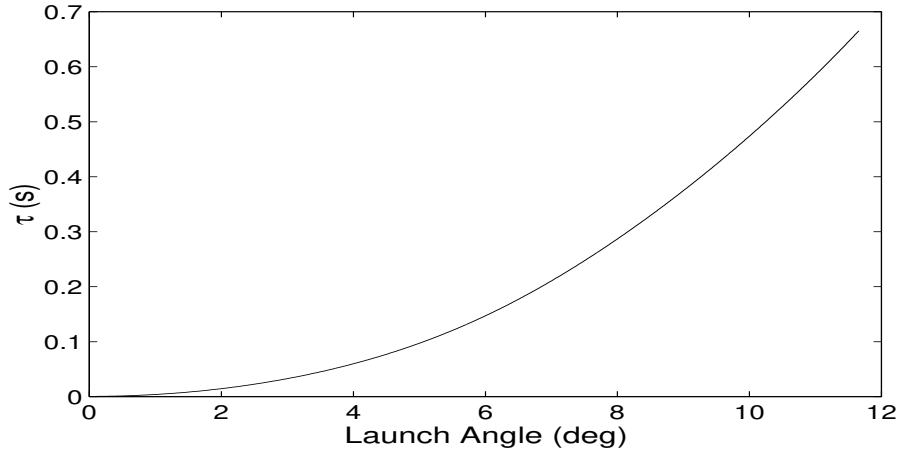


Fig. 4. Time delay $\tau = 2\pi I/\bar{c}$ versus ray launch angle.

panel. Temporal shifts between the fuzzy segments can be roughly estimated using Eqs. (36) and (37) but more accurate and detailed description can be done with Eqs. (41), (43), and (47).

4.3 Travel time differences in range-dependent waveguide

To check the accuracy of Eqs. (41) and (43) we have considered eigenrays connecting the point source and an observation point at 1000 km range set at a depth of 0.5 km. An eigenray with the launch angle $\chi = 5.1^\circ$ and the identifier +44 has been arbitrary chosen as a reference one. Its travel time has been compared with that of 24 other eigenrays whose starting and arriving momenta differ from that of the reference ray by no more than ± 0.015 . This restriction has been imposed to ensure closeness of starting and final points (in phase plane) of compared rays. Although the trajectories of all these eigenrays look similar near the source and near the observation point, at intermediate ranges they can differ significantly. This is seen in the upper panel of Fig. 5 where the trajectories of the reference eigenray (thin solid line) and one of the eigenrays with the identifier +46 (thick solid line) are shown. Range dependencies of action variables of these rays are presented in the lower panel.

The differences in travel times of the reference eigenrays and other eigenrays are presented in Fig. 6. The points depict the differences obtained by ray tracing, while the circles show predictions made with Eq. (41) (upper row of plots) and with Eq. (43) (lower row of plots).

In the left column of plots we compare the reference eigenray with eigenrays having the same identifier, +44. In the right column we make comparison with eigenrays whose identifiers are +46 (rays 18 through 21), +48 (ray 23), and +50 (ray 24). It is seen that Eq. (41) gives poor estimations for differences in travel times of eigenrays with the same identifier but it does much better for eigenrays whose numbers of cycles differ by 1, 2, and 3. Equation (43) provides

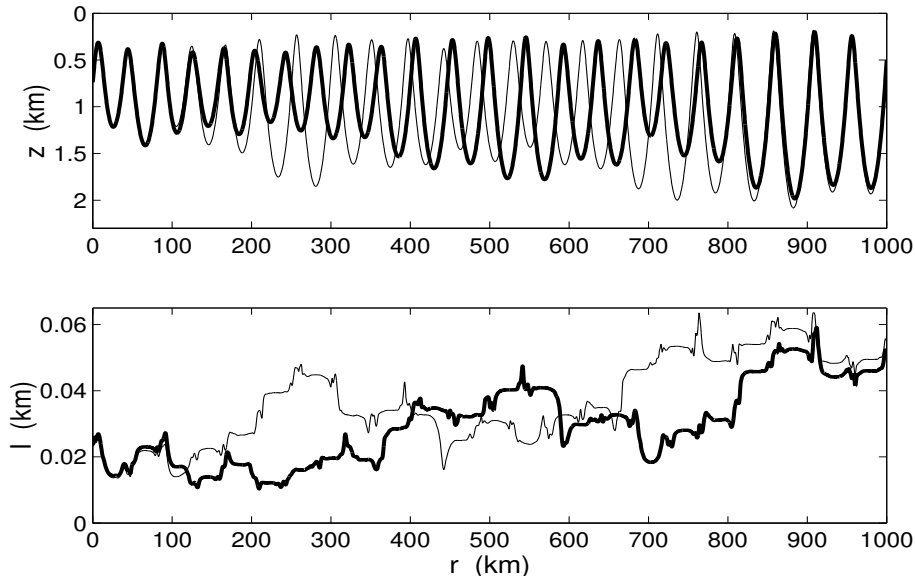


Fig. 5. The reference eigenray with the identifier +44 (thin solid) and one of the eigenrays with the identifier +46 (thick solid). Upper panel: trajectories. Lower panel: action variables as functions of range.

good predictions for all the eigenrays.

4.4 Dispersion and bias of the timefront segment due to inhomogeneities

4.4.1 Two mechanisms of ray travel time variations due to the perturbation

Equation (47) relates travel times of a ray in the range-dependent (perturbed) waveguide and another ray in the range-independent (unperturbed) waveguide. For short, we shall call these rays the perturbed ray and the unperturbed ray. Neglecting small terms including Δz_s and Δz_e , rewrite Eq. (47) in the form

$$\Delta t = 2\pi N \bar{I} / \bar{c} + \delta t_I + \delta t_V, \quad (50)$$

where

$$\delta t_I = \frac{1}{2\bar{c}} \int \omega'(\bar{I}) \Delta I^2 dr, \quad (51)$$

$$\delta t_V = \frac{1}{\bar{c}} \int dr \left(\sqrt{n^2(r, z(r)) - p^2(r)} - \sqrt{n_0^2(z(r)) - p^2(r)} \right), \quad (52)$$

and consider the case $N = 0$ when both perturbed and unperturbed rays have the same number of cycles, i.e. the same topology. In both Eqs. (51) and (52) the integration goes along the trajectory of **perturbed** ray, defined by the

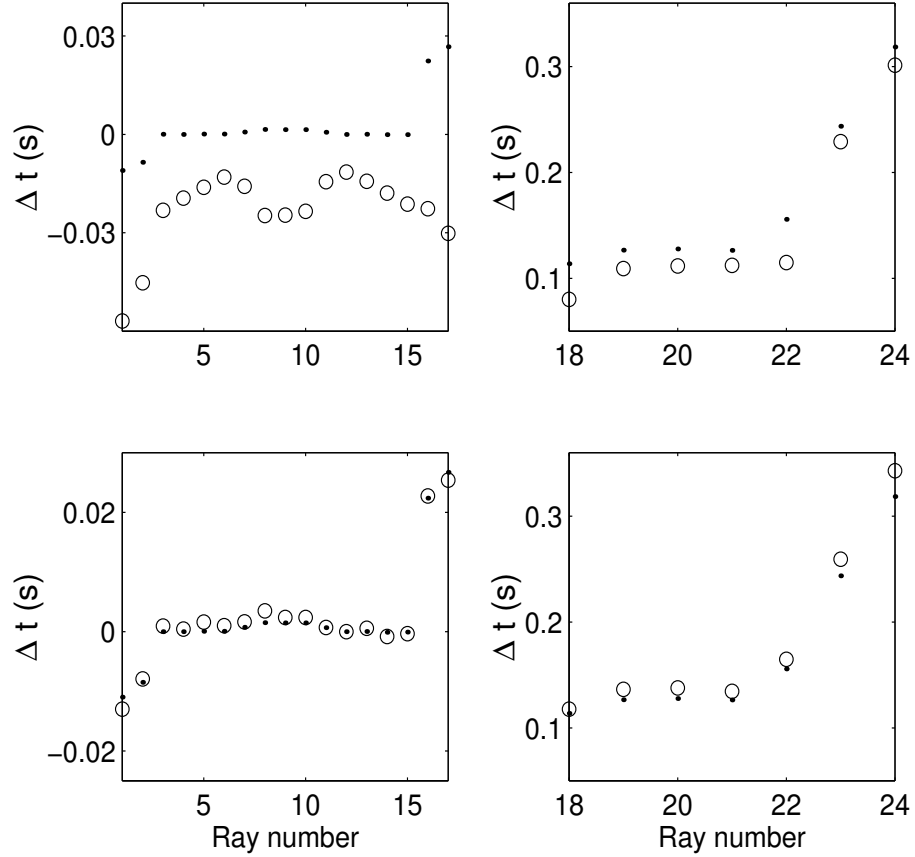


Fig. 6. Differences in travel times between the reference eigenray and 24 other eigenrays obtained with ray tracing (points) and predicted (circles) by Eqs. (41) (upper row of plots) and (43) (lower row of plots). In the left column of plots the reference ray is compared to other eigenrays with the same identifier +44, while in the right column it is compared to eigenrays with identifiers +46 (rays 18 through 21), +48 (ray 23), and +50 (ray 24).

equations $z = z(r)$ and $p = p(r)$. The difference Δt can be interpreted as a travel time shift due to perturbation.

According to Eq. (50), Δt is a sum of two terms: δt_I and δt_V . The term δt_V represents a difference in time delays of signals propagating along the ray path in the perturbed waveguide (in which this path satisfies the ray equations) and along the same path formally placed in the unperturbed waveguide. In other words, δt_V can be interpreted as a travel time shift due to variations of the refractive index along the trajectory. Then, δt_I can be considered as a travel time shift due to change of the trajectory shape.

It is interesting that, typically, the shifts δt_I and δt_V have opposite signs. In deep sea acoustic waveguides the cycle length is usually increases with the grazing angle at which the ray intersects the sound-channel axis. It means that the derivative $\omega'(I)$ should be predominantly negative because the action variable grows with the launch angle (see Figs. 3 and 4). So, the value of δt_I should be, typically, negative. In our particular environmental model, ω' is negative for all rays that do not reflect off the surface and, so, for such rays δt_I is always negative.

In contrast, the value of δt_V turns out to be mostly positive, although it is not so evident from Eq. (52). We have discovered this surprising fact in our numerical calculations (see results presented below) and do not know how general it is. However, we suppose that such a situation may be typical. This expectation is based on the following reasons.

Grazing angles of rays playing important role in long range sound propagation are small. Therefore $|p|$ is always substantially less than n and, approximately,

$$\bar{c}\delta t_V \simeq f(r) = \int_0^r dr(n(r, z(r)) - n_0(z(r))). \quad (53)$$

Consider the three derivatives of f with respect to r :

$$\begin{aligned} \frac{df}{dr} &= n - n_0, \quad \frac{d^2 f}{dr^2} = \frac{\partial(n - n_0)}{\partial z} \frac{dz}{dr}, \\ \frac{d^3 f}{dr^3} &= \frac{\partial(n - n_0)}{\partial z} \frac{d^2 z}{dr^2} + \frac{\partial^2(n - n_0)}{\partial z^2} \left(\frac{dz}{dr}\right)^2. \end{aligned} \quad (54)$$

Assuming that the dependence of the refractive index (even perturbed) on the horizontal coordinate, r , is much smoother than its dependence on the vertical coordinate z , we have neglected partial derivatives with respect to r .

In the small-angle approximation ray equations (6) and (7) reduce to

$$\frac{d^2 z}{dr^2} = n \frac{\partial n}{\partial z}.$$

Substituting it in Eq. (54) and taking into account that z -dependence of n is much more detailed than that of n_0 we drop derivatives of n_0 in Eq. (54) and, finally, get

$$\frac{d^3 f}{dr^3} \simeq n \left(\frac{\partial n}{\partial z}\right)^2 + \frac{\partial^2 n}{\partial z^2} \left(\frac{dz}{dr}\right)^2. \quad (55)$$

For simplicity we assume that the reference sound speed \bar{c} has been chosen to make the value of n close to 1. Then, the terms $n(\partial n/\partial z)^2$ and $|\partial^2 n/\partial z^2|$ are of the same order. On the other hand, $|dz/dr| \ll 1$ which means that the first term on the right hand side of Eq. (55) dominates. So, the third derivative of f with respect to r should be mostly positive. For this reason we may expect positiveness of δt_V , at least, at long ranges where the integration will smooth out fluctuations in the integrand of (53) and the positiveness of the third derivative will have a chance to reveal itself.

Let us remind that the difference δt_V has been defined here using the integration over the trajectory of the **perturbed** ray. We cannot predict the sign of the eikonal shift due to weak variations of refractive index if the traditional definition given by Eq. (53) with integration over the **unperturbed** ray path [1, 22, 23] is used.

4.4.2 Bias of the timefront segment

Equation (47) (or (50)) provides a tool to study the variations of the time front segment due to the perturbation. To illustrate this point consider the rays with the identifier +45. The portions of timefronts formed by these rays shown in different panels of Fig. 3 are presented in the same plot in Fig. 7. It is clearly seen that the scattering of points depicting arrivals in the presence of the perturbation has some regular bias: rays in the perturbed waveguide, on average, arrive earlier than that in the unperturbed one. In Fig. 8 we compare predictions made with Eq. (47) with exact values of Δt . This has been done in the following way.

Each perturbed ray arriving at the depth z belonging to the interval from 0.4 to 1.6 km (there are 590 such rays), has been compared to the unperturbed ray having the arrival depth closest to z . Both rays were taken from the fans described above. In the upper panel of Fig. 8 the points depict predictions of the travel time difference between the perturbed and unperturbed rays made with Eq. (47). The difference for every pair of such rays is plotted against their arrival depth z . Exact values of these differences obtained by ray tracing, are connected by the thin solid line. In the lower panel the same results are presented after some smoothing defined by the relation

$$\Delta t_{smooth}(m) = T^{-1} \sum_{m'} e^{-(m-m')^2/\Delta m^2} \Delta t(m), \quad T = \sum_{m'} e^{-(m-m')^2/\Delta m^2}. \quad (56)$$

All the pairs of rays have been sorted by arrival depth of the perturbed ray and $\Delta t(m)$ is the difference for the m -th pair. The points and the thin solid line in the lower panel of Fig. 8 show Δt_{smooth} 's obtained by smoothing the results presented in the upper panel with the smoothing scale $\Delta m = 10$. It is seen that Eq. (47) gives a good prediction for the smoothed travel time shift.

In Fig. 9 we can see contributions to the travel time shifts from the terms δt_I (circles) and δt_V (points). All the δt_I 's are negative while most of the δt_V 's,

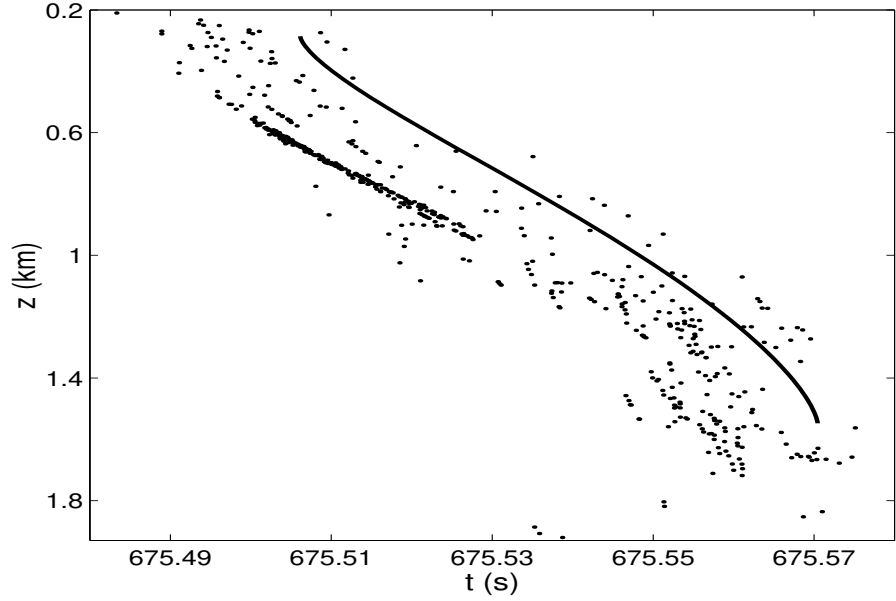


Fig. 7. Arrival of rays with the identifier +45 in the unperturbed (solid line) and perturbed (points) waveguides. Fragments of the timefronts presented in the upper and lower panels of Fig. 3 are shown here in the same plot.

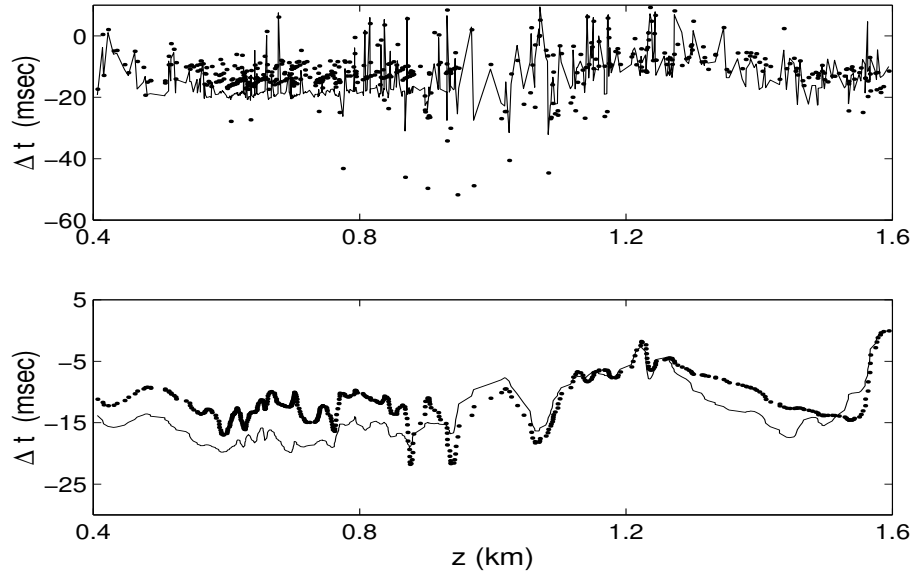


Fig. 8. Upper panel: travel time shifts due to the perturbation for rays with the identifier +45 (thin solid line) and estimations of these shifts predicted by Eq. (47) (points). Lower panel: the same after smoothing according to Eq. (56) with the smoothing scale $\Delta m = 10$.

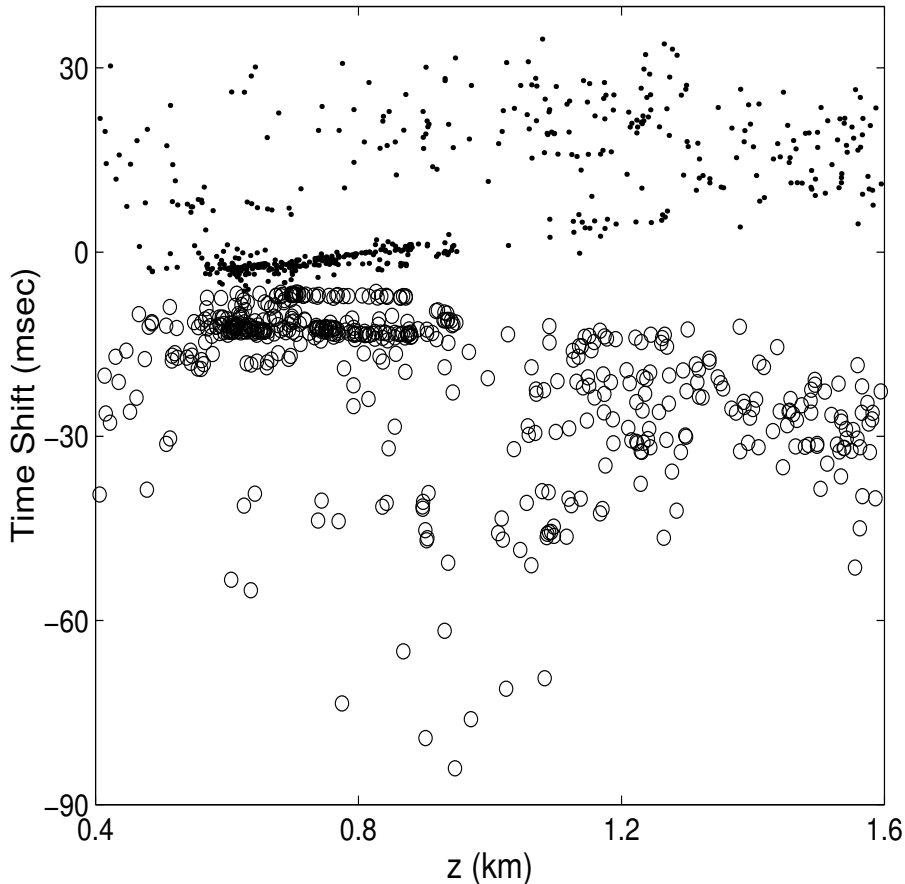


Fig. 9. Components of the travel time shift due to the perturbation, δt_V (points) and δt_I (circles), for rays with the identifier +45 versus arrival depth.

consistent with our expectation, are positive. Furthermore, we see that, on average, $|\delta t_I| > |\delta t_V|$, which means that the main mechanism of the travel time shift is related to the trajectory deviations from its unperturbed shape. This mechanism defines the sign of the bias of the segment considered.

However, for the axial rays forming the latest portion of the timefront in the lower panel of Fig. 3 the situation is opposite. These rays are not chaotic and shifts of their travel times due to inhomogeneities are determined mainly by the mechanism related to sound speed variations along ray paths. Unlike the previous example, in this case $\Delta t \approx \delta t_V > 0$ and the near axial rays in the presence of the perturbation arrive later than in the unperturbed waveguide. Equation (52) provides a good estimation of the corresponding bias which is about 0.01 s.

4.4.3 On stability of timefront segments

The timefront segment is not completely destroyed by the perturbation if

$$|\Delta t| = |\delta t_I + \delta t_V| < \tau = 2\pi I_{seg}/\bar{c} \quad (57)$$

for rays contributing to the segment. The symbol I_{seg} denotes some characteristic value of action variables of these rays. We already know the values of δt_V for rays with the identifier +45 and that for rays forming the latest portion of the timefront. The values computed for other fan rays are also mostly positive and typically less than 0.05 s. Looking at Fig. 4 we see that for not very small launch angles

$$\delta t_V \ll \tau. \quad (58)$$

This means that the main mechanism leading to distortion of the timefront segment is related to trajectory deviations from its unperturbed shape. On the other hand, for segments formed by steep rays the travel time shifts, δt_I , are also small compared to the corresponding values of τ . Such segments are distinguishable in Fig. 3 and in this sense they are stable.

Another manifestation of this property has been discovered by Tappert and Tang [8] (see also Ref. [10]). They have demonstrated numerically that in the presence of a weak range-dependent inhomogeneity leading to ray chaos, the unperturbed eigenray usually splits into a cluster of eigenrays whose arrivals are relatively closely spaced in time.

The smallness of δt_I can be qualitatively interpreted from the viewpoint of Hamilton's (Fermat's) principle. Indeed, going back to Sec. 2.2.2 we can rewrite δt_I in the form

$$\delta t_I = \frac{1}{\bar{c}}[S_0(P) - S_0(U)] \quad (59)$$

where $S_0(P)$ and $S_0(U)$ are the values of the functional $S_0 = \int(pdz - H_0 dr)$ evaluated over the trajectories of perturbed (P) and unperturbed (U) rays, respectively. According to Fermat's principle, the ray U in the unperturbed waveguide is a stationary path of the functional S_0 . The absence of linear in ΔI terms in Eqs. (47) and (51) is a consequence of this principle. Since ΔI is our small parameter, vanishing of the first order term in this parameter gives some qualitative interpretation of the timefront segment stability.

5 Range-dependent unperturbed waveguide

An ocean-acoustic propagation model in the form of a superposition of a range-independent sound speed profile and a weak range-dependent perturbation responsible for emergence of ray chaos, is often too idealized. In this section we shortly outline how the above results can be generalized to a more realistic model in which a weak perturbation, δc , is imposed on a smooth range-dependent sound speed field, c_0 , i.e.

$$c(r, z) = c_0(r, z) + \delta c(r, z). \quad (60)$$

First, consider another way of introducing the action-angle variables in the range-dependent waveguide [14] without dividing the Hamiltonian into the sum of an unperturbed term and a perturbation. Let us define canonical transformations (13) and (14) at every range r using Eqs. (17) and (18) evaluated for an auxiliary range-independent waveguide with the same cross-section that the real waveguide has at the current range. In this case the canonical transformation will be different at different ranges and Eqs. (13) and (14) translate to

$$I = I(p, z, r), \quad \theta = \theta(p, z, r) \quad (61)$$

and

$$z = z(I, \theta, r), \quad p = p(I, \theta, r). \quad (62)$$

The generating function G now becomes a function of not only I and z , but of r , as well. However, $H = -\sqrt{n^2 - p^2}$ in the new variables is a function of I and r , but not θ [14].

Since the transformation to (I, θ) variables is canonical, the Hamilton equations retain their canonical form

$$\frac{dI}{dr} = -\frac{\partial H_s}{\partial \theta}, \quad \frac{d\theta}{dr} = \frac{\partial H_s}{\partial I} \quad (63)$$

with the new Hamiltonian [14]

$$H_s(I, \theta, r) = H(I, r) + \Lambda(I, \theta, r), \quad (64)$$

where

$$\Lambda(I, \theta, r) = \left. \frac{\partial G(I, z, r)}{\partial r} \right|_{z=z(I, \theta, r)}. \quad (65)$$

The term Λ is small and can be neglected if range variations in the environment are adiabatic, i.e. if they are small at the cycle of the ray trajectory. Then, according to the first of Hamilton equations (63) I remains constant along the ray trajectory, i.e. the action variable defined in this way does have a property of adiabatic invariance.

However, we suppose that the above approach is not convenient for description of chaotic rays. The point is that in this case Λ is not negligible, the connection between H , Λ and δc is non-trivial, and it is difficult to divide Hamiltonian (64) into a sum of a smooth unperturbed term and a small perturbation. But such a decomposition is needed for application of our perturbation theory.

A more appropriate approach can be developed if the unperturbed waveguide with $c(r, z) = c_0(r, z)$ is adiabatic. Then, it is convenient to introduce the action-angle variables at every range r using an auxiliary range-independent waveguide with the cross-section coinciding with that of the unperturbed waveguide. This yields the new Hamiltonian in the form

$$H_s = H_0(I, r) + V(I, \theta, r), \quad (66)$$

where $V(I, \theta, r)$ is the perturbation defined in Eq. (25) with the unperturbed refractive index n_0 now depending not only on z but on r , as well. Then the Hamilton equations look almost the same

$$\frac{dI}{dr} = -\frac{\partial V}{\partial \theta}, \quad (67)$$

$$\frac{d\theta}{dr} = \omega(I, r) + \frac{\partial V}{\partial I} \quad (68)$$

as Eqs. (28) and (29) in Sec. 2.2.2, although the angular frequency $\omega(I, r) = \partial H_0(I, r)/\partial I$ now depends on r .

The derivation of expressions for differences in ray travel times presented in Sec. 3 can be easily generalized to the waveguide model considered here. It turns out that in the case of adiabatic unperturbed waveguide, Eqs. (36), (41), (43), and (47) remain valid.

6 Summary

Ray travel times in acoustic waveguides have been studied by applying the Hamiltonian formalism in terms of the action-angle variables. Comparatively simple analytic relations (36), (41), (43), and (47) for differences in travel times of two rays starting from two closely spaced points in phase plane and arriving at other two closely spaced points, have been obtained. The use of these equations have been demonstrated in numerical simulations carried out for a model of a deep sea waveguide with inhomogeneities induced by internal waves. By comparing to results of ray tracing, our approximate formulas have been shown to work well, at ranges up to 1000 km in spite of chaotic behavior of ray trajectories. Numerical simulations for longer ranges have not yet been performed.

In the range-independent waveguide the difference in eigenray travel times is given by surprisingly simple approximate relation (37) [19]-[21]. It establishes a kind of conservation law: the temporal shifts between the neighboring timefront segments formed by the rays with launch angles (action variables) close to some given value χ_0 ($I(\chi_0)$) does not depend on range and up to a multiplicative constant are close to $I(\chi_0)$. It allows one to estimate differences between neighboring segments of the timefront by simple evaluation of the action variable as a function of the launch angle. Note, that terms similar to (37) are also present in Eqs. (43) and (47). Moreover, these terms give main contributions to the differences Δt if the rays under consideration have different numbers of cycles. So, Eq. (37) may give crude estimations of temporal intervals between time front segments in the perturbed waveguide as well, unless the segments are completely destroyed by the perturbation.

The relations obtained in this paper allows one to compare travel times of rays propagating in the same waveguide as well as that of rays propagating in different waveguides. In particular, by comparing rays from the perturbed and

unperturbed waveguides we have studied travel time shifts due to the perturbation and corresponding variations in the timefront. (See Refs. [22, 23] for a more traditional approach for description of the travel time shifts).

We argue that the use of the action-angle variables gives an insight into mechanisms of travel time variations. The travel time shift due to the perturbation, Δt , has been presented as a sum of two constituents, δt_V and δt_I . The constituent δt_V is associated with sound speed variations along the trajectory, while δt_I is interpreted as a shift caused by variations of the trajectory shape. Our approach gives analytic expressions for both terms. It has been shown that in case of weak inhomogeneities induced by internal waves these terms usually have different signs ($\delta t_V > 0$, $\delta t_I < 0$), and for most rays the mechanism related to trajectory shape variations dominates, i.e. the perturbation results in decrease of travel times. For steep rays the value of δt_I turns out to be small compared to the differences in time between neighboring segments of the unperturbed timefront. This property means stability of the early portion of the timefront with respect to the perturbation. It has been qualitatively interpreted from the viewpoint of Fermat's (Hamilton's) principle.

Equations (41), (43), and (47) can be applied for studying of travel time shifts due to other types of inhomogeneities such as mesoscale inhomogeneities or that induced by large-scale seasonal or climatic variations in the environment. However, in the present paper this issue has not been addressed.

The expressions we have derived in this paper yield a comparatively simple connection between ray travel times and action variables, i.e. between different characteristics of rays. However, what is needed for solving inverse problems are simple formulas relating ray characteristics to the environmental parameters to be reconstructed. We hope that Eqs. (41), (43), and (47) can be used for obtaining such relations. The first step in this direction should be developing of a perturbation approach (proceeding from ray equations (28) and (29)) to establish connection between range variations of the action and fluctuations in the environment. This important topic deserves a special investigation and has not been broached here.

Our main formulas (36), (41), (43), and (47) remain valid for the ray theory taken in the parabolic equation (small angles) approximation, although the explicit expressions for the Hamiltonian, eikonal and other ray characteristics will change their forms. The most important of these formulas are presented in the Appendix.

Acknowledgment

I thank Prof. G. Zaslavsky for benefit of our discussions on problems of quantum and wave chaos. I am grateful to Dr. I.P. Smirnov whose ray code has been used for numerical simulations. The work was supported by the U.S. Navy Grant N00014-97-1-0426 and by the Grant No. 00-02-17402 from the Russian Foundation for Basic Research.

Appendix. Hamiltonian formalism corresponding to the parabolic equation

So far, we have considered the Hamiltonian formalism corresponding to full wave theory. A similar formalism can be derived proceeding from the standard parabolic equation [3, 6, 9]. Here we present expressions defining the unperturbed Hamiltonian, the perturbation and the generating function of the canonical transformation to the action-angle variables.

In the parabolic equation approximation, or small-angle approximation, the connection between the momentum, p , and the ray grazing angle, χ , is given by

$$p = dz/dr = \tan \chi. \quad (69)$$

Expression (5) for the eikonal remains valid but the explicit expression for the Hamiltonian now takes the form

$$H = \frac{p^2}{2} + U(r, z), \quad U(r, z) = \frac{1}{2} (1 - n(r, z)^2). \quad (70)$$

This yields the Hamilton equations

$$\frac{dz}{dr} = p, \quad \frac{dp}{dr} = -\frac{\partial U}{\partial z}. \quad (71)$$

In a range-independent waveguide with $U = U_0(z)$ and $H = H_0 = p^2/2 + U_0$, an analog to the energy conservation law (Snell's law), $H_0 = \text{const}$, again establishes a simple relation between the momentum, p , and coordinate, z :

$$p = \pm \sqrt{2(H_0 - U_0(z))}. \quad (72)$$

The action variable, I , as a function of "energy" H_0 is now defined by the integral

$$I = \frac{1}{2\pi} \oint p dz = \frac{1}{\pi} \int_{z_{\min}}^{z_{\max}} dz \sqrt{2(H_0 - U_0(z))}. \quad (73)$$

Equation (11) remains valid but the explicit expression for the cycle length transforms to

$$D = 2 \int_{z_{\min}}^{z_{\max}} \frac{dz}{\sqrt{2(H_0 - U_0(z))}}. \quad (74)$$

The generating function for the canonical transformation to the action-angle variable is now

$$G(I, z, r) = \begin{cases} \int_{z_{\min}}^z dz \sqrt{2[H_0(I) - U_0(z)]}, & p > 0 \\ 2\pi I - \int_{z_{\min}}^z dz \sqrt{2[H_0(I) - U_0(z)]}, & p < 0 \end{cases}, \quad (75)$$

and the canonical transformation is defined by

$$p = \frac{\partial G}{\partial z} = \pm \sqrt{2[H_0(I) - U_0(z)]}, \quad (76)$$

$$\theta = \frac{\partial G}{\partial I} = \begin{cases} \frac{2\pi}{D} \int_{z_{\min}}^z \frac{dz}{\sqrt{2[H_0(I) - U_0(z)]}}, & p > 0 \\ 2\pi I - \frac{2\pi}{D} \int_{z_{\min}}^z \frac{dz}{\sqrt{2[H_0(I) - U_0(z)]}}, & p < 0 \end{cases} . \quad (77)$$

Finally, we note that for the range-dependent perturbation to the unperturbed Hamiltonian, Eq. (25) now translates to

$$V(r, z) = U(r, z) - U_0(z).$$

References

- [1] W. Munk and C. Wunsch. "Ocean acoustic tomography: A scheme for large scale monitoring," *Deep-Sea Res.* **26**, 123-161 (1979).
- [2] J. Spiesberger and K. Metzger. "Basin-scale tomography: a new tool for studying weather and climate," *Journal of Geophysical Research*, **96**, 4869-4889 (1991).
- [3] S.S. Abdullaev and G.M. Zaslavskii, "Classical nonlinear dynamics and chaos of rays in wave propagation problems in inhomogeneous media," *Usp.Phys.Nauk* **161**(8), 1-43 (1991).
- [4] D.R. Palmer, M.G. Brown, F.D. Tappert, and H.F. Bezdek, "Classical chaos in nonseparable wave propagation problems," *Geophys. Res. Lett.*, 1988, **15**, 569-572 (1988).
- [5] M.G. Brown, F.D. Tappert, G. Goni, "An investigation of sound ray dynamics in the ocean volume using an area preserving mapping," *Wave motion* **14**, 93-99 (1991).
- [6] K.B. Smith, M.G. Brown, and F.D. Tappert, "Ray chaos in underwater acoustics," *J. Acoust. Soc. Am.*, **91**, 1939-1949 (1992).
- [7] K.B. Smith, M.G. Brown, and F.D. Tappert, "Acoustic ray chaos induced by mesoscale ocean structure," *J. Acoust. Soc. Am.* **91**, 1950-1959 (1992).
- [8] F.D. Tappert and X. Tang. "Ray chaos and eigenrays," *J. Acoust. Soc. Am.*, **99**, 185-195 (1996).
- [9] J. Simmen, S.M. Flatte, and G.-Y. Wang, "Wavefront folding, chaos, and diffraction for sound propagation through ocean internal waves," *J. Acoust. Soc. Am.*, **102**, 239-255 (1997).
- [10] J.L. Spiesberger and F.D. Tappert, "Kaneohe acoustic thermometer further validated with rays over 3700 km and the demise of the idea of axially trapped energy," *J. Acoust. Soc. Am.*, **99**, 173-184 (1996).
- [11] P. F. Worcester, B. D. Cornuelle, M. A. Dzieciuch, W. H. Munk, B. M. Howe, J. A. Mercer, R. C. Spindel, J. A. Colosi, K. Metzger, T. Birdsall and A. B. Baggeroer, "A test of basin-scale acoustic thermometry using a

- large- aperture vertical array at 3250-km range in the eastern North Pacific Ocean,” J. Acoust. Soc. Am. **105**, 3185-3201 (1999).
- [12] J. A. Colosi, E. K. Scheer, S. M. Flatté, B. D. Cornuelle, M. A. Dzieciuch, W. H. Munk, P. F. Worcester, B. M. Howe, J. A. Mercer, R. C. Spindel, K. Metzger, T. Birdsall and A. B. Baggeroer, “Comparisons of measured and predicted acoustic fluctuations for a 3250-km propagation experiment in the eastern North Pacific Ocean,” J. Acoust. Soc. Am. **105**, 3202-3218 (1999).
- [13] G.M. Zaslavsky. *Physics of chaos in Hamiltonian systems* (Imperial College Press, Singapore, 1998).
- [14] L.D. Landau and E.M. Lifshits, *Mechanics* (Nauka, Moscow, 1973).
- [15] M. Born, E. Wolf, *Principles of optica*, (Pergamon Press, Oxford, 1965).
- [16] S.S.Abdullaev, *Chaos and dynamics of rays in waveguide media*. Edited by G.Zaslavsky (Gordon and Breach science publishers, 1993).
- [17] L.M.Brekhovskikh and Yu.Lysanov, *Fundamentals of Ocean Acoustics* (Springer-Verlag, Berlin, 1991).
- [18] F.B. Jensen, W.A. Kuperman, M.B. Porter, and H. Schmidt, *Computational Ocean Acoustics* (AIP, Woodbury, New York, 1994).
- [19] A.L. Virovlyanskii, “Travel times of acoustic pulses in the ocean,” Sov. Phys. Acoustics, **31(5)**, 399-401 (1985).
- [20] W.Munk and C.Wunsch, “Ocean acoustic tomography: rays and modes,” Rev. Geophys. and Space. Phys., **21(4)**, 1-37 (1983).
- [21] A.L. Virovlyansky, “On general properties of ray arrival sequences in oceanic acoustic waveguides,” J. Acoust. Soc. Am. **97(5)**, 3180-3183 (1995).
- [22] S.M. Flatte, R. Dashed, W.M. Munk, K.M. Watson, and F. Zakhariassen, *Sound transmission through a fluctuating ocean* (Cambridge U.P., London, 1979).
- [23] J.L. Spiesberger, “Ocean acoustic tomography: Travel time biases,” J. Acoust. Soc. Am. **77**, 83-100 (1985).